

A mathematical analysis of milling mechanics in a planetary ball mill

P.P. Chattopadhyay^a, I. Manna^a, S. Talapatra^b, S.K. Pabi^{a,*}

^a *Metallurgical and Materials Engineering Department, Indian Institute of Technology, Kharagpur, W.B. 721302, India*

^b *Applied Mechanics Department, Bengal Engineering College (deemed university), Howrah, W.B. 711103, India*

Received 25 January 2000; received in revised form 10 April 2000; accepted 22 April 2000

Abstract

A detailed mathematical analysis is presented to advance the current understanding of the mechanics of milling operation in a planetary ball mill in terms of a global Cartesian reference space. The ab initio calculations have identified the role of milling parameters in determining the condition of detachment of the ball from the vial wall. The condition of an 'effective' impact has been identified in terms of the vial-to-disk speed ratio. It emerges from the analysis that the role of velocity components of the ball at the instant of its impact on the vial wall warrants proper consideration, because the tangential force determines the lower bound of the vial-to-disk speed ratio conducive for effective transfer of impact energy to the powder charge in the mill. Finally, a comparison of the experimental results of grain size reduction during milling of elemental Fe and Cu–Al powder blend with the similar predictions of the present analysis demonstrates for the first time that elastic properties of the balls and vials play an important role in determining the rate of structural refinement during ball milling. © 2001 Elsevier Science B.V. All rights reserved.

Keywords: Dynamics; Kinematics; Mechanical alloying; Modeling; Planetary ball milling

1. Introduction

Mechanical alloying (MA) is a versatile route of solid state synthesis of nanometric novel materials with metastable microstructure and composition [1]. It is known that high energy ball milling in a planetary mill leads to MA of the constituent powders through a process involving repeated deformation, fragmentation and cold welding [1]. In the past, several attempts have been made to simulate the dynamics of this milling process in terms of ball velocity, frequency of impact and power/kinetic energy transferred to the powder charge during milling [2–14]. Maurice and Courtney [2] and Courtney [3] have simulated the mechanics of milling on the basis of Hertzian criterion of perturbed impact to predict the volume of material affected per impact, impact duration, strain/strain-rate, temperature rise and cooling rate. Both these analyses deal with the phenomenological aspects of collision between two balls and/or a ball and vial wall rather than the kinematics of the ball motion. On the other hand, Burgio et al. [4] have derived a set of kinematic equations to compute the velocity and acceleration of a ball in a planetary mill, and thereby, estimate the energy transferred to the powder particles. The ball distribution inside the vial is considered to be independent of the kinematics of the ball

motion. However, the analysis does not provide a governing principle to predict an optimum milling condition.

Subsequently, Abdellaoui and Gaffet [5], Gaffet [6] and Gaffet et al. [7] have suggested through more rigorous analyses that the power of ball impact rather than the kinetic energy or frequency may determine the end products and efficiency of the milling process. These models, however, overlook some important kinematic parameters like the angular variation of impact velocity in determining the effective amount of power/energy transferred to the powder particles during a given collision event. In this regard, Besset et al. [8] have proposed that the impact velocity may be experimentally determined from the size of indentation on a metallic surface. Magini and Iasonna [9], Iasonna and Magini [10] and Magini et al. [11] have considered the same kinematic conditions earlier proposed by Burgio et al. [4], and calculated the energy transferred per impact to compare the latter with the experimentally determined electrical/mechanical power consumed. In spite of such an elegant approach, the analysis have not yielded an optimum condition of milling in terms of power/energy for a given MA condition. Watanabe et al. [12] have simulated the kinematics and related trajectory of the ball motion for a variety of ball mill devices using Kelvin's dashpot-spring model. The analysis as well as the photographic observation of ball trajectory suggest that the relative direction of rotation between the disk and vial (i.e. parallel and counter rotation)

* Corresponding author. Tel.: +91-3222-83272; fax: +91-3222-55303.
E-mail address: skpabi@metal.iitkgp.ernet.in (S.K. Pabi).

determines the nature of ball trajectory, i.e. cataracting and cascading motion, respectively.

Subsequently, Dallimore and McCormick [13] have predicted the grinding media motion in a planetary ball mill by a two-dimensional discrete element method of computer analysis. They have compared the Kelvin and Maxwell visco-elastic models and elastic/plastic yield model, to characterize the normal and tangential impacts. In addition, they have also considered the variation in ball motion and energy dissipation during collision for varying milling condition in terms of the CuO/Ni reaction synthesis [13]. Regarding the nature of collision, Le Brun et al. [14] have expressed the collision events and their effectiveness for MA through a kinematic parameter (R_{critical}) without defining its significance in terms of the mechanism of collision. It is apparent from the earlier results [2–14] that most of the investigations conducted so far in the area of dynamics of planetary ball milling have either studied the role of total power of impact (P_t) for MA or have attempted to predict the trajectory of the ball motion within the vial. However, further investigation is warranted to explore the most conducive conditions for MA derived in terms of the milling parameters. Moreover, the influence of the impacting medium (balls and vials) in determining the kinetics of MA has not yet been theoretically analyzed.

In the present investigation, we have presented a kinematic analysis in terms of a single Cartesian reference frame for both the rotating disk and vial. The present model explicitly defines the role of milling parameters in determining the criterion for the detachment of ball from the rotating vial wall prior to impact, so that the detachment angle never assumes an unrealistic value in the subsequent analysis. For the first time, the effect of tangential component of the impact velocity of the ball at the instant of impact has also been taken into account under a no-slip condition to establish the criterion of the effective impact. Finally, the present analysis demonstrates that power consumed for elastic deformation (P_d) of the ball, which is determined by its elastic properties, warrants due consideration in the milling operation. A comparison between the experimental results and the predictions of the analysis reveals that a higher value of ($P_t - P_d$) at a comparable level of P_t results into an enhanced rate of refinement the crystallite size in elemental Fe or Cu–Al powder blend.

2. Mathematical formulation

2.1. Kinematics of motion

The present analysis of the planetary milling operation, in accordance with the earlier relevant models [4,5], considers the overall process involving a number of balls in the vial as equivalent to the cumulative effect of recurring impacts of a single ball on the vial wall. In other words, the balls are assumed not to interfere with each other's motion, and hence,

the kinematics and dynamics of a single ball could, in principle, represent the overall process of mechanical alloying (MA) in a planetary ball mill. For estimating the effect of an individual impact, the effective amount of power/energy transferred by the balls to the powder volume entrapped between the ball and vial wall needs proper evaluation. In this regard, it is assumed that the kinetic energy of impact is conserved within the colliding bodies.

Following Abdellaoui and Gaffet [5], a single ball has been conceived as a point mass moving on the vial wall under the 'no-slip' condition. In addition, the present analysis considers the ball motion as a periodic event initiating from a given point on the vial wall that offers maximum reaction force on the ball. The kinematics of ball motion, in contrast to that presented in Ref. [5], has been treated here in terms of a global reference frame having its origin (O) located at the center of the disk (Fig. 1). Here, r_d and r_v are the distances between the origin and center (C) of the vial, and the latter and a ball, respectively. The rotational speed of the disk, determined by the rotational speed of the line OC, is ω_d in the anticlockwise (or positive) direction. In accordance with the planetary motion of the mill, the rotational speed of the vial in the clockwise direction relative to the line OC is ω_v . Here $P(x_0, y_0)$ is a point on the vial surface lying on the line OC, that is taken as the point of initiation of the ball motion. At any instant t , the position vectors x_1 and y_1 (Fig. 1) of the ball at a given time (t) may be expressed as:

$$x_1 = r_d \cos \omega_d t + r_v \cos(\omega_d - \omega_v)t \quad (1)$$

and

$$y_1 = r_d \sin \omega_d t + r_v \sin(\omega_d - \omega_v)t \quad (2)$$

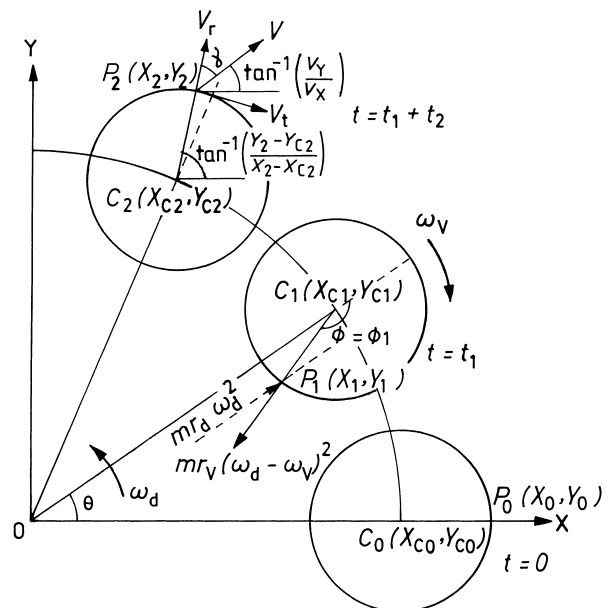


Fig. 1. Schematic diagram showing positions of the ball on the vial surface at the point of initiation of its motion (at $t=0$), detachment (at $t=t_1$) and collision ($t=t_1+t_2$) (see text).

Consequently, the respective velocity components in the x and y directions, i.e. v_x and v_y , may be obtained as:

$$v_x = \frac{dx_1}{dt} = -\omega_d r_d \sin \omega_d t - (\omega_d - \omega_v) r_v \sin(\omega_d - \omega_v) t \quad (3)$$

and

$$v_y = \frac{dy_1}{dt} = \omega_d r_d \cos \omega_d t + (\omega_d - \omega_v) r_v \cos(\omega_d - \omega_v) t \quad (4)$$

2.2. Detachment criterion

Resolution of the centrifugal force originating from the rotation of the vial and disk along the direction P_1C_0 in Fig. 1 yields the net reaction (N) acting on the ball at a given position on the vial wall as:

$$N = m [r_v(\omega_d - \omega_v)^2 + r_d \omega_d^2 \cos \phi] \quad (5)$$

where ϕ is the angular distance described by the ball at a given moment during its motion on the vial wall starting from P_0 in Fig. 1, and m the mass of a ball. Initiating its motion from P_0 , the ball remains in contact with the vial wall as long as N is positive. This condition yields (from Eq. (5)):

$$\cos \phi \geq -\frac{r_v(\omega_d - \omega_v)^2}{r_d \omega_d^2} \quad (6)$$

At the point of detachment, i.e. at $\phi = \phi_1$, the resultant reaction on the ball is reduced to zero, i.e. $N=0$. As a consequence, it is evident from Eq. (6) that:

$$\cos \phi_1 = -\frac{r_v(\omega_d - \omega_v)^2}{r_d \omega_d^2} \quad (7)$$

It may be noted that a similar expression has been obtained in an earlier analysis [5]. However, the limiting value of $\cos \phi$ (≥ -1) expressed by Eq. (7) is utilized here to define a detachment parameter (S) as:

$$S = \frac{r_v(\omega_d - \omega_v)^2}{r_d \omega_d^2} \quad (8)$$

Since S must be confined within the limit $0 \leq S \leq 1$, it can dictate the possible values/combination of ω_d and ω_v for a given mill (i.e. known values of r_v and r_d) such that the ball is detached from the vial wall at a given point to make an impact at some other point on the vial wall considering the condition expressed by Eq. (7) at the point of detachment:

$$\phi_1 = \pi - \cos^{-1} S \quad (9)$$

According to Fig. 1, the interval between the ball moving from the position $P_0(x_0, y_0)$ to $P_1(x_1, y_1)$ on the vial surface can be obtained as $t_1 = \phi_1 / \omega_v$. In the same interval, if θ_1 is the angular displacement of the line OC , then $\theta_1 = \phi_1 \omega_d / \omega_v$. At the moment of detachment, the position of the ball $P_1(x_1, y_1)$

is a point on the surface of the vial with its center located at (x_{c1}, y_{c1}) . Hence,

$$(x_1 - x_{c1})^2 + (y_1 - y_{c1})^2 = r_v^2 \quad (10)$$

where, $x_{c1} = r_d \cos \theta_1$ and $y_{c1} = r_d \sin \theta_1$.

2.3. Kinematics of impact

After the detachment event, the ball continues to move in a given trajectory and its position at successive time steps is calculated from the components of velocity in the direction of coordinate axes at the moment of detachment. The unaccelerated motion of the ball continues for an interval t_2 until it collides with the vial surface (Fig. 1). The time step is restricted such that the distance of the ball center from the vial wall at the final step, say Δr_v , should be less than the ball radius. Position of collision on the vial surface, $P_2(x_2, y_2)$, is given by:

$$x_2 = x_1 + v_x t_2 \quad (11)$$

and

$$y_2 = y_1 + v_y t_2 \quad (12)$$

Considering the position of the ball at the point of detachment, and subsequent collision in terms of the respective position of the center of the vial

$$(x_1 + v_x t_2 - x_{c2})^2 + (y_1 + v_y t_2 - y_{c2})^2 = (x_1 - x_{c1})^2 + (y_1 - y_{c1})^2 \quad (13)$$

where x_{c2} and y_{c2} are the position coordinates of the centre of the vial at the instant of collision (Fig. 1). Substituting, $(x_{c1}^2 + y_{c1}^2)$, $(x_{c2}^2 + y_{c2}^2)$, x_{c2} and y_{c2} obtained in terms of r_d , Eq. (13) can be rewritten (for $t_2 > 0$) as:

$$(v_x^2 + v_y^2)t_2^2 + 2(x_1 v_x + y_1 v_y)t_2 - 2\{x_1 r_d \cos(\phi_1 + \omega_d t_2) + y_1 r_d \sin(\phi_1 + \omega_d t_2)\} - 2\{v_x r_d \cos(\phi_1 + \omega_d t_2) + v_y r_d \sin(\phi_1 + \omega_d t_2)\}t_2 + 2(x_1 x_{c1} + y_1 y_{c1}) = 0 \quad (14)$$

It is interesting to note here that only at $P_1(x_1, y_1)$ and $P_2(x_2, y_2)$ the ball remains attached to the vial wall and Eq. (14) is satisfied. At any other point on the trajectory of the ball during t_2 , the left-hand side of Eq. (14) would yield a negative value, indicating that the ball does not remain attached to the vial. In the event of a collision, the resultant velocity (v) of impact of the ball is obtained from Eq. (14) as:

$$v^2 = \omega_d^2 r_d^2 + (\omega_d - \omega_v)^2 r_v^2 + 2\omega_d(\omega_d - \omega_v)r_v r_d \cos \phi_1 = v_r^2 + v_t^2 \quad (15)$$

where v_r and v_t , respectively, are the radial and tangential components of impact velocity and the angle of incidence (γ) in Fig. 1 is expressed as:

$$\gamma = \tan^{-1} \left(\frac{v_t}{v_r} \right) = \tan^{-1} \left(\frac{y_2 - y_{c2}}{x_2 - x_{c2}} \right) - \tan^{-1} \left(\frac{y_1}{x_1} \right) \quad (16)$$

2.4. Re-initiation of ball motion

After an impact, the ball needs to move to a point situated at the vial surface on the line OC for initiating the next cycle. The time elapsed (t_3) for this motion is given by:

$$t_3 = \frac{\alpha}{\omega_v} \quad (17)$$

where $\alpha = [2\pi - (\phi_1 + \omega_v t_2)]$.

2.5. Frequency of impact

The total time for a complete cycle of ball motion is determined by the time through which the ball is in contact on the vial wall (t_1), the interval between a detachment and subsequent reattachment to the vial wall (t_2), and the time elapsed between a collision and subsequent initiation of the next cycle of motion (t_3). Time period for one complete cycle may thus be expressed as:

$$t_f = t_1 + t_2 + t_3 \quad (18)$$

Hence, frequency of collision is given by:

$$f = \frac{1}{t_f} \quad (19)$$

2.6. Dynamics of ball impact

Considering that the ball does not change its velocity during a flight along the free path, the available kinetic energy (E_t) of the ball of mass (m) in the event of an impact is expressed as:

$$E_t = 0.5 mv^2 \quad (20)$$

Thus, the total power (P_t) transmitted by the ball per impact is obtained as:

$$P_t = fE_t \quad (21)$$

Some of the earlier studies [13,14] have considered the ball–vial collision to take place under a Hertzian impact condition [15], and in the present analysis too, this condition has been adopted. Considering a circular area of impact, the radial component of the impact force, from the Hertzian impact theory [15], can be obtained as:

$$F_r = \left(\frac{4}{3}\right) r_b^{1/2} \left(\frac{Y}{1-\nu^2}\right) \delta_r^{3/2} \quad (22)$$

where r_b is the ball radius, δ the approach distance of the ball toward the vial surface, Y the elastic modulus, and ν the Poisson's ratio. Hence, the normal pressure (p_n) is obtained as:

$$p_n = \frac{F_r}{\pi a^2} \quad (23)$$

where a is the radius of the circular impact area obtained from Ref. [15]. If the deformation of the ball is taken to

be reversible in nature, the duration of impact (t_i) can be obtained from Ref. [15] as:

$$t_i = 2.94 \frac{\delta_r}{v_r} \quad (24)$$

Hence, taking the reversible nature of impact into account, the compression time may be obtained as $t_c = t_i/2$.

In the present analysis, the mass and radius of curvature of the vial are considered to be infinity relative to those of the ball. Thus, a suitable modification of the expression for linear momentum in the tangential direction yields [15]:

$$F_t = m \frac{d}{dt} (v_t + \omega_r r_b) \quad (25)$$

where F_t is the tangential component of the impact force, v_t the tangential component of the velocity at the point of collision, and ω_r the relative angular velocity. Similar modification for the conservation of the moment of the momentum [15] of the ball about the axis normal to the plane of motion passing through the point of impact yields:

$$\frac{d}{dt} [mv_t r_b + m(r_b^2 + r_g^2)\omega_r] = 0 \quad (26)$$

Here, r_g is the radius of gyration of the ball about its center of mass. Eliminating ω_r from Eqs. (25) and (26), F_t can be obtained as:

$$F_t = -\frac{m}{(1 + r_b^2/r_g^2)} \left(\frac{dv_t}{dt_i}\right) \quad (27)$$

Considering F_t to be operative throughout the interval t_c to bring the tangential velocity down to zero, Eq. (27) yields:

$$\int_0^{t_c} dt_i = -(F_t) \frac{m}{(1 + r_b^2/r_g^2)} \int_{v_t}^0 dv \quad (28)$$

Therefore, F_t can be obtained by integrating Eq. (28) to give:

$$F_t = \frac{m}{(1 + r_b^2/r_g^2)} \left(\frac{v_t}{t_c}\right) \quad (29)$$

3. Experimental

In order to determine the influence of milling parameters on the kinetics of MA, ball milling of +300 mesh size, elemental Fe powder and a powder blend of nominal composition (expressed in atomic percentage) $\text{Cu}_{82}\text{Al}_{18}$ has been performed in a Fritsch Pulverisette P5 planetary ball mill with individual constituents having a purity level of >99.5 wt.%. In order to investigate the role of elastic properties of the milling media, ball milling of the same weight of powder (20 g) has been conducted separately in: (a) in chrome steel vials of $r_v=75$ mm using balls with $m_b=4.2$ g and $Y=2.1 \times 10^{11}$ GPa at $\omega_d=300$ and 260 rpm; and (b) WC vials of $r_v=75$ mm and balls of $m_b=8.4$ g and $Y=7.04 \times 10^{11}$ GPa at $\omega_d=240$ rpm. Grain size (d_c) variation has been determined from the broadening of the X-ray

diffraction (XRD) peaks obtained from samples collected at different stages of milling using the Scherrer equation [16].

While, instrumental broadening has been corrected by subtracting the broadening obtained from the annealed (at 600°C for 2 h) coarse grained ($>50 \mu\text{m}$) sample from the observed broadening, the contribution of strain to line broadening was eliminated by a Lorentzian curve fitting exercise [17]. However, the determination of the variation of solubility of Al in Cu for $\text{Cu}_{82}\text{Al}_{18}$ composition as a function of t has not been included in the present study. This is due to the fact that several factors, other than the milling parameters, are known to interfere in the variation of lattice parameter of a given element, e.g. the grain size itself [18,19] as well as contamination from the milling media or milling environments [20]. In fact, theoretical and experimental analyses have shown that a significant rate of alloying in the MA process is achieved only after d_c is brought down to $<100 \text{ nm}$ [21] and, hence, the variation of d_c with t can well represent the effectiveness of milling condition.

4. Results and discussion

4.1. Detachment criterion

It is known that, for a given vial (r_v) and disk radius (r_d), the main process variables for MA in a planetary mill are ω_v and ω_d [2]. Earlier attempts to construct the milling maps in terms of ω_v and ω_d using the experimental results of microstructural evolution during MA have aimed at identifying the optimum milling conditions for generating the desired microstructure [5–7]. The present mathematical analysis of the milling dynamics aims at predicting the milling condition in terms of ω_d and ω_v , for the occurrence of the most effective impact between the ball and vial wall to achieve MA.

In the present analysis, the values of r_d , r_v and ball radius (r_b) are taken as 132, 35 and 5 mm, respectively (typical of a planetary mill), unless otherwise stated. In order to define the periodicity of the ball motion, it is assumed that the ball initiates its motion from a point of maximum resultant centrifugal force on the vial surface, i.e. $P_0(x_0, y_0)$ in Fig. 1. The displacement of the ball on the vial wall is traced through an iterative computation ($\Delta t = 10^{-5} \text{ s}$) method using Eqs. (1) and (2) until the detachment condition (at position P_1 in Fig. 1) laid down by Eq. (7) is satisfied. Subsequently, the motion of the ball is monitored until the ball undergoes an impact (position P_2 in Fig. 1) satisfying the condition in accordance with Eq. (13). The velocity of the ball at the points P_1 and P_2 are obtained from Eq. (15). It may be noted that although a similar relation as that expressed in Eq. (7) has been derived in some earlier analyses [5,14], the limiting value of $\cos \phi$ imposed in the present treatment enables the prediction of a detachment criteria in terms of the milling parameters that would ascertain whether detachment of the

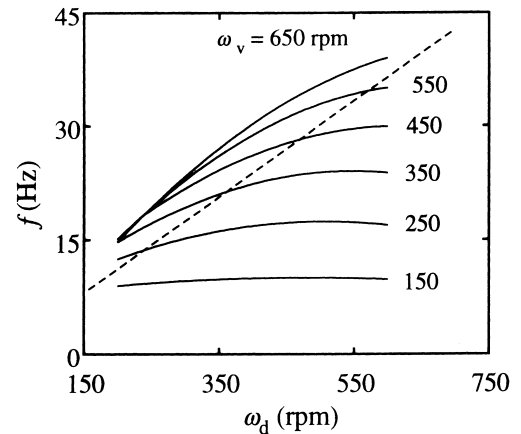


Fig. 2. Variation of f as a function of ω_d for different levels of ω_v . The broken line corresponds to $\omega_v/\omega_d=1$.

ball from the vial surface has taken place before analyzing any collision event. The milling conditions compelling the ball to remain attached to the vial surface throughout the cycle of its motion need to be avoided for an effective MA.

4.2. Frequency of impact

In this analysis, the total time (t_f) for a complete cycle of ball motion can be computed through Eq. (18). Hence, the frequency (f) of impact for a single ball may easily be obtained from Eq. (19). From the present analysis, it is found that f increases with ω_d (Fig. 2) in a manner similar to that reported by Abdellaoui and Gaffet [5]. Both these analyses indicate that f gradually approaches a plateau, the level of which increases with ω_v (Fig. 2). Here, it is also interesting to note that f increases with ω_d as long as $(\omega_v/\omega_d) > 1$ for a given level of ω_v . As (ω_v/ω_d) is reduced below unity, f gradually approaches the plateau and this transition is delineated by the broken line in Fig. 2. Thus, the present analysis predicts that the level of f is determined both by ω_d and ω_v , but the limiting value of f is determined by ω_v/ω_d ratio.

4.3. Kinetic energy and power

Fig. 3 presents the variation of total kinetic energy (E_t) as a function of ω_d obtained from Eq. (20). It is interesting to note that E_t manifests a monotonic increase with ω_d , but is insensitive to variation in ω_v . In other words, the total kinetic energy per impact seems to depend primarily on ω_d which is in accordance with the earlier prediction by Abdellaoui and Gaffet [5].

Fig. 4 records the variation of total power (P_t) estimated through Eq. (21) as a function of ω_d at different levels of ω_v . Since $P_t = E_t f$, the functional relationships between P_t (or E_t) with ω_d are similar. However, P_t , unlike E_t , is not independent of ω_v , particularly at $\omega_d > 200 \text{ rpm}$, which may be attributed to the influence of ω_v on f . In this regard, the value of P_t obtained in the present analysis using the identi-

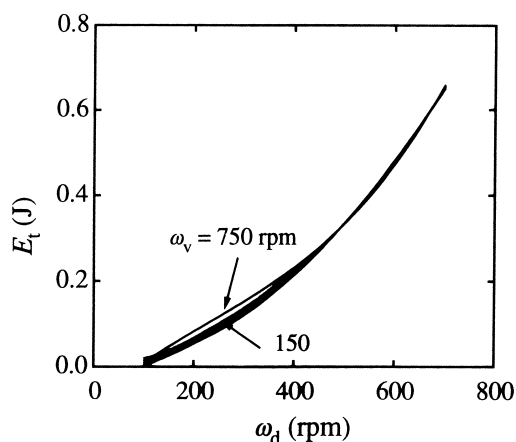


Fig. 3. Variation of E_t as a function of ω_d for different levels of ω_v .

cal milling parameters as that reported in Fig. 4 of Ref. [7] for $r_v=33$ mm has been compared with the same (Fig. 5a). It is apparent from Fig. 5a that the results obtained from the present analysis (solid lines) is in good agreement with that obtained from Ref. [7] despite a slight difference in the method of calculation of t_f . However, with decreasing value of r_v , only a marginal divergence in the value of P_t is obtained in the present analysis in contrast to the significant difference in the same reported in Ref. [7]. Similarly, it is evident from Fig. 5b that the theoretical and experimental results presented by Magini and Iasonna [9] manifest reasonable agreement with the results of the present study under comparable conditions; although the magnitude of P_t predicted by the present model is consistently lower than that predicted by them. This difference may originate from the fact that the experimental value of P_t obtained by Magini and Iasonna [9] corresponds to the power input to the mill by a mechanical device, while P_t in the present study signifies the cumulative power of impact obtained from the planetary motion of the balls which does not include

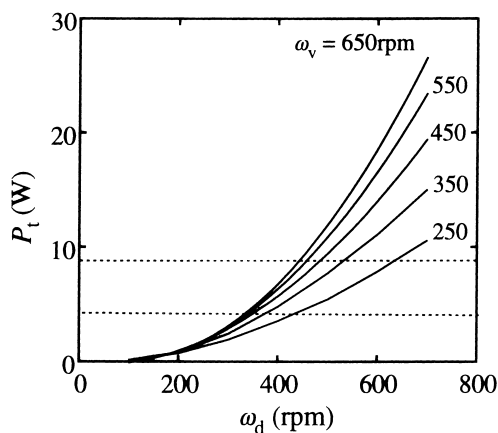


Fig. 4. Variation of P_t as a function of ω_d at different levels of ω_v . The dotted lines represent the range of P_t required for amorphization of Ni-Zr by mechanical alloying (as reported by Abdellaoui and Gaffet [5]).

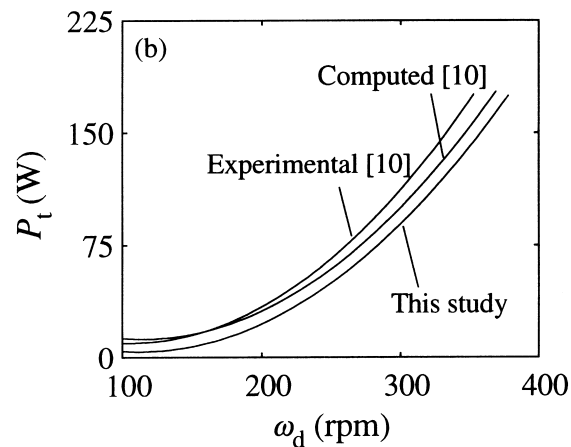
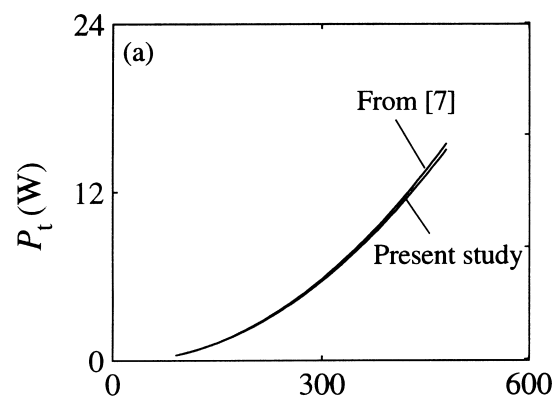


Fig. 5. (a) Variation of P_t as a function of ω_d and its comparison with the same reported by Gaffet et al. [7]. (b) Variation of P_t as a function of ω_d and its comparison with the same (both predicted and experimental results) as reported by Iasonna and Magini [10] under comparable conditions of milling.

any frictional loss of energy in the power transmission system.

4.4. Direction of impact

Earlier, Le Brun et al. [14] have considered the angle of impact in a qualitative manner by classifying the different modes of interaction between the ball and vial wall (i.e. impact and frictional) in terms of (ω_v/ω_d) . The present analysis attempts to examine more thoroughly the role of the angle of incidence (γ) of the ball on the vial wall (cf. Fig. 1). The variation of γ with (ω_v/ω_d) in Fig. 6 demonstrates that γ is oriented in the anticlockwise (positive) direction for $(\omega_v/\omega_d) < 1$, which is in the reverse sense to that of ω_v (clockwise). At $(\omega_v/\omega_d) = 1$, the incidence is normal to the vial surface, i.e. $\gamma = 0$. For $(\omega_v/\omega_d) > 1$, γ is oriented in clockwise (negative) direction and is parallel to that of rotation of the vial (clockwise) at the point of incidence. The variation of γ with (ω_v/ω_d) (as noted in Fig. 6) manifests its influence on the variation of the radial (F_r) and tangential

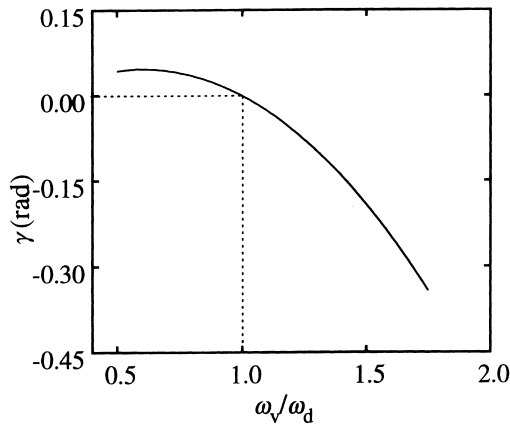


Fig. 6. Variation of γ as a function of ω_v/ω_d at $\omega_d=400$ rpm. Note that $\gamma=0$ at $\omega_v/\omega_d=1$.

(F_t) components of the impact force, as shown in Fig. 7. It is evident from Fig. 7a that F_r does not show significant variation with (ω_v/ω_d) at any given ω_d ; but increases substantially with an increase in ω_d . However, the direction of F_r is insensitive to that of γ . On the other hand, F_t continually decreases with (ω_v/ω_d) , and it changes its sign from positive to negative at $(\omega_v/\omega_d)=1$ (Fig. 7b). It may be noted that Eq. (7) yields $\phi=90^\circ$ at $\omega_v=\omega_d$ (i.e. r_v is perpendicular to OC in Fig. 1). Similarly, Eq. (15) yields $v=\omega_d r_d$ for $(\omega_v/\omega_d)=1$, i.e. perpendicular to OC. Thus, it appears that the ball, when detached from vial wall at $\phi=90^\circ$, moves along r_v , and subsequently undergoes an impact normal to the vial surface. This prediction is at variance with the value

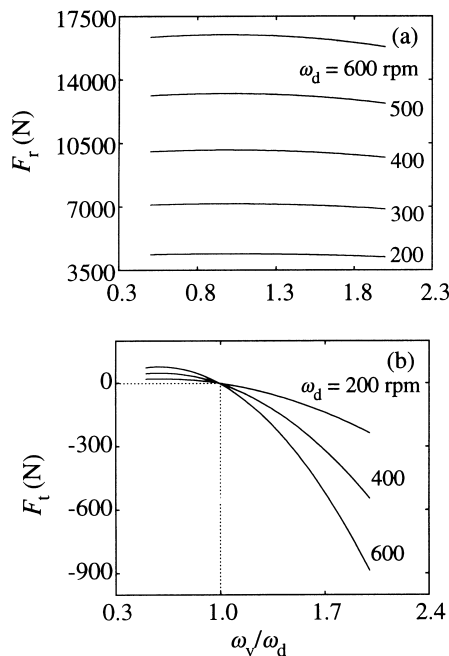


Fig. 7. (a) Variation of F_r as a function of ω_v/ω_d for different levels of ω_d . (b) Variation of F_t as a function of ω_v/ω_d for different levels of ω_d . Note that $F_t=0$ for $\omega_v/\omega_d=1$ for all levels of ω_d .

of $(\omega_v/\omega_d)=2.26$ quoted by Le Brun et al. [14] for a pure (i.e. radial) impact. However, it is not possible to identify the origin for such a difference in the absence of the relevant mathematical derivation underlying similar prediction in Ref. [14].

The experimental results of Le Brun et al. [14] have been presented in terms of microhardness and morphology of deformed Cu powder as a function of (ω_v/ω_d) . Here, the higher values of microhardness have been obtained at $(\omega_v/\omega_d)=1$, though the corresponding microstructure of deformed Cu powder shows a faceted, instead of platelike, morphology. They postulated that the chaotic nature of ball motion at $(\omega_v/\omega_d)=1$ results into the dominance of the frictional mode of interaction between the ball and vial wall. However, the faceted morphology and higher microhardness of Cu powders at $(\omega_v/\omega_d)=1$, in comparison with the same at $(\omega_v/\omega_d)>1$, seems to suggest that impacts at $(\omega_v/\omega_d)=1$ are primarily of the radial type as predicted by the present analysis. At $(\omega_v/\omega_d)<1$, F_t becomes positive, because the ball spins in a direction opposite to the that of the vial. As a result, the powder particles within the impact area start sliding relative to each other in the opposite direction. Thus, the particles would tend to sweep out from the contact area between the ball and vial wall. As a result, the more positive is the F_t , the greater would be the tendency of the ball to have direct interaction with the vial surface without sufficient amount of powder particles trapped in-between. This would lead to a higher level of friction and wear induced contamination of the end product. However, when F_t acts in the same direction as that of the vial rotation for $(\omega_d/\omega_v)>1$, the ball and vial spin in the same direction. This condition is conducive for the tangential as well as normal interaction forces of impact to promote effective deformation of the entrapped powder, as predicted in [2].

4.5. Experimental validation

Earlier, several investigations have indicated that power of impact plays the governing role in determining the kinetics of MA. In this regard, Magini et al. [11] have recently demonstrated that the rate of MA remains the same when a planetary ball mill is operated in equi-power absorption conditions, in spite of allowing a large variation in the milling parameters. However, the role played by elastic properties of the impacting medium in determining such kinetics has not been taken into consideration. It may be noted that a considerable fraction of total power (P_t) generated by an impact is spent for the elastic deformation of the ball ($P_d=p_r^2 \pi r_b^2 \delta_r f / 6Y$ [2]). Thus, the effective power (P_e) transferred by the ball during an impact to the powder can be obtained as $P_e=P_t-P_d$. Naturally, P_e takes into account the elastic property of the milling media. Figs. 8 and 9 show the calculated variation of P_t and P_e , respectively, as a function of ω_d for WC and chrome steel media typically in a Fritsch P5 planetary mill having $\omega_v/\omega_d=1.25$, $r_b=10$ mm, $r_d=132$ mm, and $r_v=35$ mm. Fig. 8 reveals that an identical

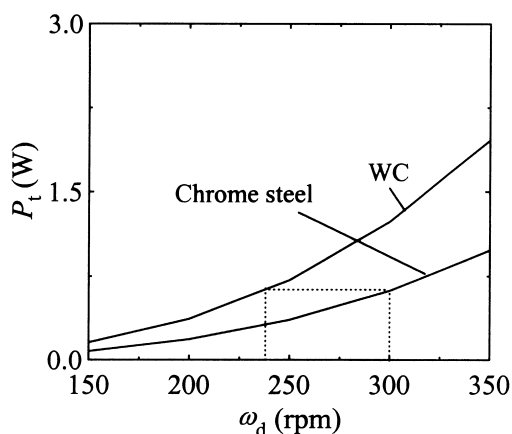


Fig. 8. Variation of P_t as a function of ω_d for WC and chrome-steel milling medium.

level of P_t can be achieved at $\omega_d=240$ rpm in a WC vial and at 300 rpm in the chrome-steel vial. Here, it is interesting to note from Fig. 9 that P_e for milling in the chrome-steel medium at 300 rpm is higher than that for WC medium at 240 rpm. However, an identical level of P_e can be achieved in WC and chrome-steel medium by milling at $\omega_d=240$ and 260 rpm, respectively. A similar comparison with respect to the normal pressure (p_n) exerted by the ball during an impact is shown in Fig. 10. It appears that p_n is at a higher level in case of WC vial than in the chrome steel vial for the range of ω_d considered here.

In an attempt to compare the effects of P_t , P_e and p_n , ball milling: (1) the first set of experiments are conducted at the identical level of P_t (cf. Fig. 8) using WC medium at $\omega_d=240$ rpm and chrome-steel medium at $\omega_d=300$ rpm; and (2) in the second set at the same level of P_e using WC medium at $\omega_d=240$ rpm and chrome-steel medium at $\omega_d=260$ rpm. The grain size (d_c) reduction data obtained as a function of milling time for elemental Fe powder and Cu in $\text{Cu}_{82}\text{Al}_{18}$ powder blend are shown in Fig. 11a and

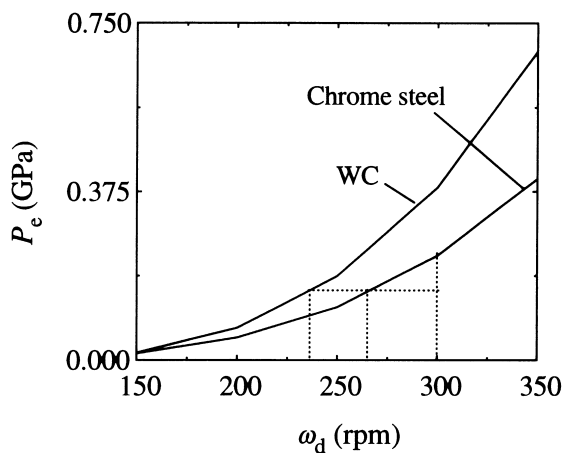


Fig. 9. Variation of P_e as a function of ω_d for WC and chrome-steel milling medium.

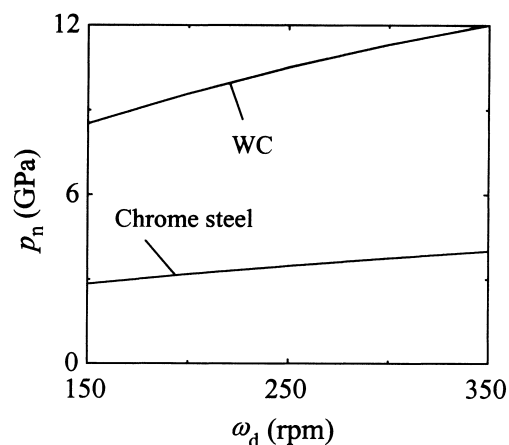


Fig. 10. Variation of p_n as a function of ω_d for WC and chrome-steel milling medium.

b, respectively. It is evident that in either case a faster rate of reduction in d_c is exhibited by the sample milled in chrome-steel vial with $\omega_d=300$ rpm than that in WC vial with $\omega_d=240$ rpm, although the level of P_t is same in either case (Fig. 8). On the other hand, a similar rate of reduction

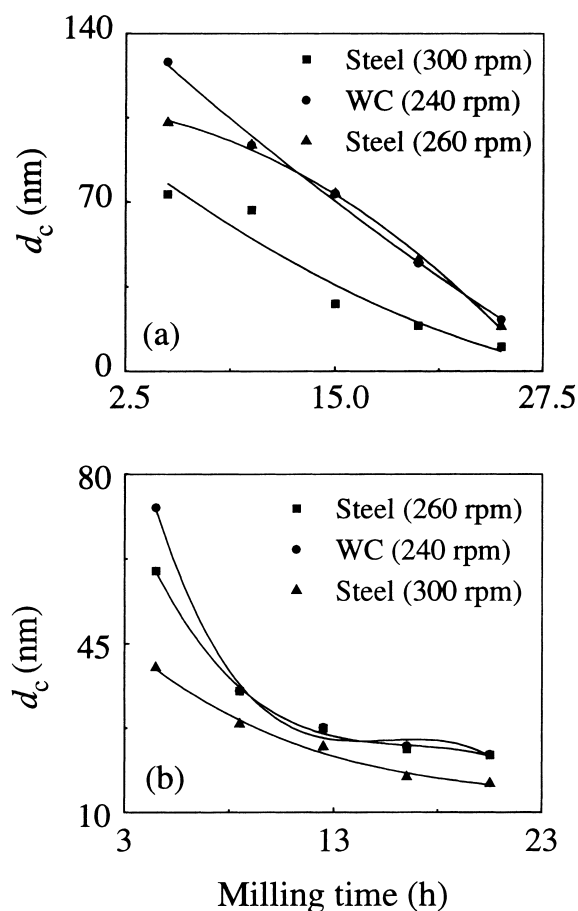


Fig. 11. Variation of d_c as a function of milling time for: (a) elemental Fe; and (b) Cu-18 at.% Al ball milled in WC and chrome-steel vials with selected levels of ω_d .

in d_c is achieved both in elemental Fe powder and for Cu in $\text{Cu}_{82}\text{Al}_{18}$ powder blend when milling is conducted at the same level of P_e , i.e. $\omega_d=240$ rpm in WC and $\omega_d=260$ rpm in chrome-steel medium, respectively (cf. Fig. 9). Thus, it appears that P_e rather than P_t , is the more appropriate criterion for determining the milling performance, and hence the elastic modulus of the milling medium warrants due consideration in the MA process. It may be noted that the higher level of elastic modulus in case of WC in comparison to that of chrome-steel vial is manifested in the value of p_n (Fig. 10). However, a faster kinetics revealed in case of chrome-steel medium at 300 rpm in comparison to that in WC medium at 240 rpm indicates that the higher level of p_n in case of the WC medium cannot ensure a faster rate of grain-size reduction during ball milling. The slower alloying kinetics in WC medium, compared to that in chrome-steel medium has earlier been observed in other alloy systems [20]. It might be postulated that Fe contamination from the steel medium may be responsible for this behavior. However, such an argument may not hold good for milling of Fe powder in steel medium, where the contamination effect is marginalized.

4.6. Critical remarks

In summary, the present analysis distinguishes itself from the earlier mathematical models of the milling mechanics by several important features. Unlike the earlier models [2–14], the present analysis explicitly defines through a detachment parameter S (Eq. (8)) the feasibility of detachment of the ball from the vial wall as an a priori function of the milling variables, to ensure that the detachment angle (ϕ_1) does not assume an unrealistic value for a ball vial impact. The nature of variation of f , E_t and P_t with the milling variables shows reasonable agreement with most of the theoretical and experimental results presented earlier in two rigorous analyses by Abdellaoui and Gaffet [5] and Magini and Iasonna [9]. In addition, the present analysis shows that spin of the ball at the instant of impact on the vial wall must be taken into consideration for identifying the effective impact conditions. It is shown that the tangential component of the impact force F_t changes its sign from positive to negative at $(\omega_v/\omega_d)=1$ (Fig. 7b). For a positive value of F_t , the ball and vial spins in the reverse direction during an impact, which would tend to sweep the entrapped powders out of the impact area. As a result, the bare contact between the ball and vial surfaces would provoke a higher level of wear and contamination, particularly at higher ω_d . On the other hand, a negative value of F_t is conducive to retaining the powder particles within the impact area. In contrast to the earlier analyses [2–14], the present one emphasizes the role played by the elastic property of the milling medium in determining the kinetics of ball milling. It is demonstrated that P_e , rather than P_t , can be a more appropriate factor influencing the milling performance.

5. Conclusions

The ab initio calculation of milling mechanics in a planetary ball mill in terms of a global Cartesian reference frame has yielded the relevant kinematic and dynamic functions associated with mechanical alloying. The important conclusions are:

1. The detachment parameter S predicts the feasibility of detachment of a ball from the vial wall in terms of the milling variables (ω_d , ω_v , r_v and r_d). The detachment, in turn, ensures the succession of impacts.
2. The values of the total power P_t computed as a function of the disk speed ω_d in the present analysis show reasonable agreement with the values of the same reported in the literature.
3. Among the various milling parameters, the disk speed ω_d seems to exert the most significant influence on the radial force that actuates deformation.
4. The direction of the tangential force dictates the effectiveness of an impact and, hence, limits the lower value of the vial-to-disk speed ratio ω_v/ω_d necessary to induce an impact conducive for ball milling.
5. Comparison with the experimental results of milling Fe and Cu–Al blend shows that an enhanced grain refinement rate is achieved with a higher level of effective power P_e even at the same level of total power P_t . However, comparable kinetics are obtained at similar values of P_e , rather than P_t . It is also noted that a much higher value of normal pressure p_n in the case of WC medium in comparison to that in the chrome-steel medium does not ensure an enhanced kinetics in the former.

Acknowledgements

This work is partially sponsored by the Department of Science and Technology, Government of India (Grant No. III.4(23)92-ET). One of the author (P.P. Chattopadhyay) gratefully acknowledges the financial support under the QIP scheme of the AICTE, New Delhi.

References

- [1] C.C. Koch, in: R.W. Cahn, P. Hassan, E.J. Kramer (Eds.), *Materials Science and Technology*, Vol. 15, VCH, Weinheim, 1991, 193 pp.
- [2] D. R. Maurice, T. H. Courtney, *Metall. Trans. A* 22 (1990) 299.
- [3] T.H. Courtney, *Mater. Trans. JIM* 37 (1995) 124.
- [4] N. Burgio, A. Iasonna, M. Magini, S. Martelli, F. Padella, *Il Nuovo Cimento* 13D (1991) 459.
- [5] M. Abdellaoui, E. Gaffet, *Acta Metall. Mater.* 44 (1995) 1087.
- [6] E. Gaffet, *Mater. Sci. Eng. A* 133 (1991) 181.
- [7] E. Gaffet, M. Abdellaoui, N. Malhouroux-Gaffet, *Mater. Trans. JIM* 36 (1995) 198.
- [8] D. Basset, P. Matteazzi, F. Miani, *Mater. Sci. Eng. A* 174 (1994) 71.
- [9] M. Magini, A. Iasonna, *Mater. Trans. JIM* 36 (1995) 123.
- [10] A. Iasonna, M. Magini, *Acta Mater.* 45 (1996) 1109.
- [11] M. Magini, C. Colella, A. Iasonna, F. Padella, *Acta Mater.* 46 (1998) 2841.

- [12] R. Watanabe, H. Hashimoto, G.G. Lee, *Mater. Sci. Eng. A* 174 (1994) 71.
- [13] M.P. Dallimore, P.G. McCormick, *Mater. Trans. JIM* 37 (1996) 1091.
- [14] P. Le Brun, L. Froyen, L. Delaey, *Mater. Sci. Eng. A* 161 (1993) 75.
- [15] K.L. Johnson, in: *Contact Mechanics*, Cambridge University Press, Cambridge, 1985.
- [16] B.D. Cullity, in: *Elements of X-Ray Diffraction*, Addison–Wesley, Reading, MA, 1975, 102 pp.
- [17] R.M. Davis, B.T. McDermott, C.C. Koch, *Metall. Trans. A* 19 (1998) 2867.
- [18] X.D. Liu, H.Y. Zhang, K. Lu, Z.Q. Hu, *J. Phys.: Condensed Matter* 6 (1994) L497.
- [19] P.P. Chatterjee, S.K. Pabi, I. Manna, *Scripta Mater.*, sent for publication.
- [20] B.S. Murty, J. Joarder, S.K. Pabi, *Nanostruct. Mater.* 7 (1996) 691.
- [21] J.Y. Huang, Y.D. Yu, Y.K. Yu, D.X. Li, H.Q. Ye, *Acta Mater.* 45 (1997) 113.